

X-ray diffraction study of lattice modulations in an underdoped $\text{YBa}_2\text{Cu}_3\text{O}_{6+x}$ superconductorZahirul Islam,^{1,*} S. K. Sinha,¹ D. Haskel,¹ J. C. Lang,¹ G. Srajer,¹ B. W. Veal,² D. R. Haeffner,¹ and H. A. Mook³¹*Advanced Photon Source, Argonne National Laboratory, Argonne, Illinois 60439*²*Materials Science Division, Argonne National Laboratory, Argonne, Illinois 60439*³*Oak Ridge National Laboratory, Oak Ridge, Tennessee 37831*

(Received 24 June 2002; published 9 September 2002)

We report a temperature-dependent increase below ~ 220 K of diffuse superlattice peaks corresponding to $\mathbf{q}_0 = (\sim \frac{2}{5}, 0, 0)$ in an underdoped $\text{YBa}_2\text{Cu}_3\text{O}_{6+x}$ superconductor ($x \approx 0.63$). These peaks reveal strong c-axis correlations involving the CuO_2 bilayers, show a nonuniform increase below ~ 220 K with a plateau for ~ 100 – 160 K, and appear to saturate in the superconducting phase. We propose that this temperature dependence of the superlattice peaks is a possible manifestation of charge stripes in the CuO_2 planes which are coupled to the oxygen-ordered superstructure.

DOI: 10.1103/PhysRevB.66.092501

PACS number(s): 74.72.Bk, 61.10.Eq, 74.25.-q

The evidence of a “pseudogap” phase in the normal state of the cuprate superconductors has been found from optical and transport measurements of the underdoped compounds (see Ref. 1, and references therein). There has been much speculation about the microscopic nature of this phase.^{2,3} One possibility is that this phase is due to ordering of a kind (e.g., “spin/charge stripes”) that competes with superconductivity and has important implications for understanding the overall phase diagrams of these cuprates. The first experimental observation of stripes was in the Nd-doped La_2CuO_4 family with neutron diffraction, where both antiphase antiferromagnetic spin stripes and the corresponding charge stripes (at twice the wavevector of the magnetic stripes) were observed.^{4,5} It is important to note that the diffraction from charge stripes (or charge-density waves) is primarily from the atomic displacements or lattice distortions associated with them. In the case of the Nd-doped compounds, the stripes are accepted to be static, stabilized by the low-temperature tetragonal structure (LTT phase) of this compound. In underdoped $\text{YBa}_2\text{Cu}_3\text{O}_{6+x}$ (YBCO) compounds, Mook *et al.*⁶ reported the existence of incommensurate spin excitations at wave vectors of $(\pm 0.1, 0, 0)$ from the $(\frac{1}{2}, \frac{1}{2}, 0)$ reciprocal-space point, which they associated with dynamic stripe fluctuations. No static spin- or charge-density waves were found with neutrons, although Mook and Doğan⁷ reported anomalies in phonons of wavevector $(\pm 0.2, 0, 0)$ or the expected wavevector for the corresponding dynamic charge stripes.

We have used high-energy synchrotron x rays to search for charge stripes in underdoped $\text{YBa}_2\text{Cu}_3\text{O}_{6.63}$, since x-ray scattering integrates over the energies of the fluctuations at the wave vectors looked at. We have observed strong lattice modulations in the CuO_2 planes with wave vector $\mathbf{q}_0 = (\sim \frac{2}{5}, 0, 0)$ that become significantly enhanced upon entry into the pseudogap phase, while scattering at twice the wavevector of the incommensurate spin fluctuations mentioned above [i.e., at $(\pm 0.2, 0, 0)$] is weak or nonexistent. We propose that this low-temperature increase of the modulations is a manifestation of charge stripes which use an underlying oxygen-ordered superstructure (see below) as a spatial template, so that their wavevector is the same as that of the ordering of the oxygen vacancies [i.e., $\mathbf{q}_0 = (\sim \frac{2}{5}, 0, 0)$].

Superconductivity in orthorhombic ($a < b < c$) YBCO arises from correlated “holes” in the CuO_2 bilayers.⁸ The hole density is controlled by tuning the oxygen stoichiometry⁹ which changes the number of oxygen atoms, or vacancies, in the CuO_x -chain planes (or ab planes). In the underdoped regime (i.e., $x \leq 0.92$) these vacancies form superstructures^{10–15} which have been calculated using an anisotropic Ising model.¹⁶ These superstructures consist of different arrangements of filled and empty chains (or chain fragments) with well-defined modulations along the \mathbf{a} axis. At $x \sim 0.63$, the modulation vector is $\mathbf{q}_0 = (\sim \frac{2}{5}, 0, 0)$, relative to the nearest Bragg point, resulting from a complex arrangement of oxygen-full and oxygen-vacant CuO_x chains (two full, one empty, one full, one empty) which run parallel to the \mathbf{b} axis.¹⁴ Although observed transition temperatures of these superstructures are typically above 300 K,^{10,14,17} Monte Carlo simulations¹⁶ predict additional “branching phases” to appear as $T \rightarrow 0$ if the sample is annealed at sufficiently low temperature.¹⁶ However, transformation between these phases have been monitored with a variety of techniques (i.e., diffusion, internal friction, resistivity, and superconducting T_c , Raman spectroscopy, Hall measurements, and photoconductivity). Relaxation times resulting from a temperature change universally show an activated behavior, with an activation energy of ~ 1 eV and a prefactor in the range of $(1-5) \times 10^{-12}$ sec.^{18,19}

In this paper, we report diffuse peaks due to lattice modulations of an oxygen-ordered phase in underdoped YBCO superconductor that become significantly more intense when the sample is cooled to cryogenic temperatures. It seems highly unlikely that this intensity change could result from ordering associated with development of branching phases. Substantial intensity changes are observed as the temperature is cooled below ~ 220 K; at this temperature, the Arrhenius plot would project that the relaxation time is more than 1000 years (compared to ~ 20 h at 300 K), and increases exponentially with further cooling. Unless the activated behavior becomes entirely different in the low-temperature regime, there is no possibility of observing low-temperature changes associated with spontaneous oxygen ordering. In the present experiments, we find that diffuse peaks characterizing the oxygen-ordered phase become increasingly stronger when cooled to ~ 14 K (in < 2 h).

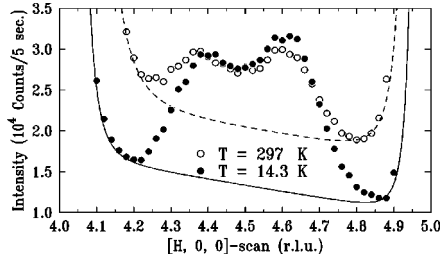


FIG. 1. Comparison of diffuse scattering at room temperature and 14.3 K, respectively, showing a clear enhancement at low temperature. Solid lines show a modeling of the background (see the text).

X-ray scattering experiments were performed at the Advanced Photon Source, Argonne National Laboratory. A set of well-annealed, self-flux-grown¹⁹ crystals was characterized on the SRI CAT 1-ID beamline using a Weissenberg camera with 65-keV x rays. A rectangular, twinned crystal ($\sim 1000 \times 300 \times 70 \mu\text{m}^3$) that showed no obvious signs of diffraction peaks from extraneous phases was chosen from the set. The magnetization measurements of this sample (annealed at ~ 300 K for several weeks) revealed T_c to be 60 K with a transition width of ~ 0.5 K, suggesting a high degree of compositional homogeneity in the bulk of the sample. Most of the present work was carried out on the SRI CAT 4-ID beamline using 36-keV x rays. A Si-(1, 1, 1) reflection was used as a monochromator with the undulator fifth harmonic tuned to provide maximum flux at this energy. The sample was cooled in a closed-cycle He refrigerator. The temperature-dependent measurements were carried out on warming from low temperature. Y fluorescence was carefully monitored to normalize to the same diffracting volume at every temperature.

The primary direction of interest in the reciprocal space is \mathbf{a}^* (i.e., the direction along the shorter Cu-O-Cu links in the CuO_2 planes and perpendicular to the CuO_x chains⁸) along which oxygen-ordering superlattice peaks appear and phonon line-broadening peaks have been reported.⁷ Figure 1 shows reciprocal-lattice scans (i.e., $[H, 0, 0]$ scans) between (4, 0, 0) and (5, 0, 0) Bragg peaks, respectively, at two different temperatures. Two broad superlattice peaks associated with a modulation vector of $\mathbf{q}_0 = (\sim \frac{2}{5}, 0, 0)$ are clearly observed at both temperatures. We note that there appears to be *no* significant scattering above the diffuse tails near the expected incommensurate charge-fluctuation peaks at $(\sim 4.2, 0, 0)$ and $(\sim 4.8, 0, 0)$, respectively.⁷ Furthermore, at the lower temperature, a series of systematic scans along \mathbf{a}^* with different values of K revealed diffuse peaks corresponding to \mathbf{q}_0 , with no signs of peaks related to $(\sim 0.2, 0, 0)$. In addition, considering the possibility of staggering of the charge fluctuations between the CuO_2 planes within a bilayer, we have collected scans along \mathbf{a}^* , with L values ranging from -2 to 0 in increments of 0.2 . No clear signs of peaks at $H \approx 4.2$ or at $H \approx 4.8$, respectively, were found in these scans either.

The intensities (corrected for background) of the \mathbf{q}_0 peaks are of the order of ~ 500 – 3500 counts/sec at 14.3 K, some $\sim 10^6$ – 10^7 orders of magnitude weaker than those of the

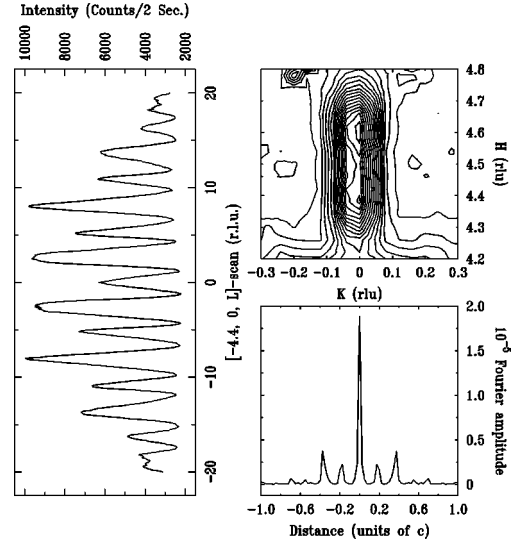


FIG. 2. Top right: Two-dimensional scan showing the extent of diffuse scattering in the $[H, K, 0]$ zone. Left: The modulation of $[-4.4, 0, 0]$ diffuse peak along \mathbf{c}^* . Lower right: The Fourier transform showing distances between planes that are correlated. All the data were collected at 14.3 K.

Bragg peaks. They are due to local lattice distortions,^{20,13} which at high temperatures have been associated with oxygen-vacancy ordering as the lattice relaxes around the vacancies. The contribution of an atomic displacement $\delta \mathbf{u}$ to the diffuse scattering amplitude at a momentum transfer \mathbf{Q} varies as $\mathbf{Q} \cdot \delta \mathbf{u}$. A series of $[H, 0, L]$ scans, with H ranging from 0.1 to 0.9 collected for a given L value of $6, 7,$ or 8 , respectively, did not show any significant scattering around $(\sim \frac{2}{5}, 0, L)$, implying that $\delta \mathbf{u} \parallel \mathbf{c}$ is small. Further, the absence of any significant scattering around $(0, 8, 0) + \mathbf{q}_0$ suggested $\delta \mathbf{u} \perp \mathbf{b}$. Indeed, a series of $[H, 0, 0]$ scans revealed that

$$\frac{I(\mathbf{G} + \mathbf{q}_0)}{I(\mathbf{G} - \mathbf{q}_0)} \propto \frac{|\mathbf{G} + \mathbf{q}_0|^2}{|\mathbf{G} - \mathbf{q}_0|^2},$$

where I is the intensity at a $\mathbf{Q} = \mathbf{G} \pm \mathbf{q}_0$ and \mathbf{G} is a reciprocal-lattice vector, confirming that the lattice distortions are predominantly longitudinal ($\delta \mathbf{u} \parallel \mathbf{a}$).

Figure 2 (top-right panel) shows a two-dimensional mesh revealing the extent of the diffuse scattering in the $[H, K, 0]$ zone. The profile is elongated along \mathbf{a}^* with two concentrated summits at $(4.4, 0, 0)$ and $(4.6, 0, 0)$, respectively. The width of the peaks along \mathbf{b}^* is much sharper (~ 0.05 r.l.u.) than that along \mathbf{a}^* (~ 0.20 r.l.u.), suggesting a slightly longer-range correlation (~ 30 Å) along the CuO_x chains than the correlation (~ 7 Å) along \mathbf{a} . Such an anisotropy of the correlation lengths within the ab plane is consistent with the quasi-one-dimensional nature of the underlying distortions. We note that we have eliminated the ambiguity between $(\frac{2}{5}, 0, 0)$ and $(0, \frac{2}{5}, 0)$, respectively, due to twinning (also see Refs. 12 and 13). All the diffuse peaks are equidistant from the nearest $(H, 0, 0)$ Bragg peak, and the splittings of the $(H, 0, 0)$ peaks and the corresponding $(0, H, 0)$ peaks from the twin were well resolved in our current setup.

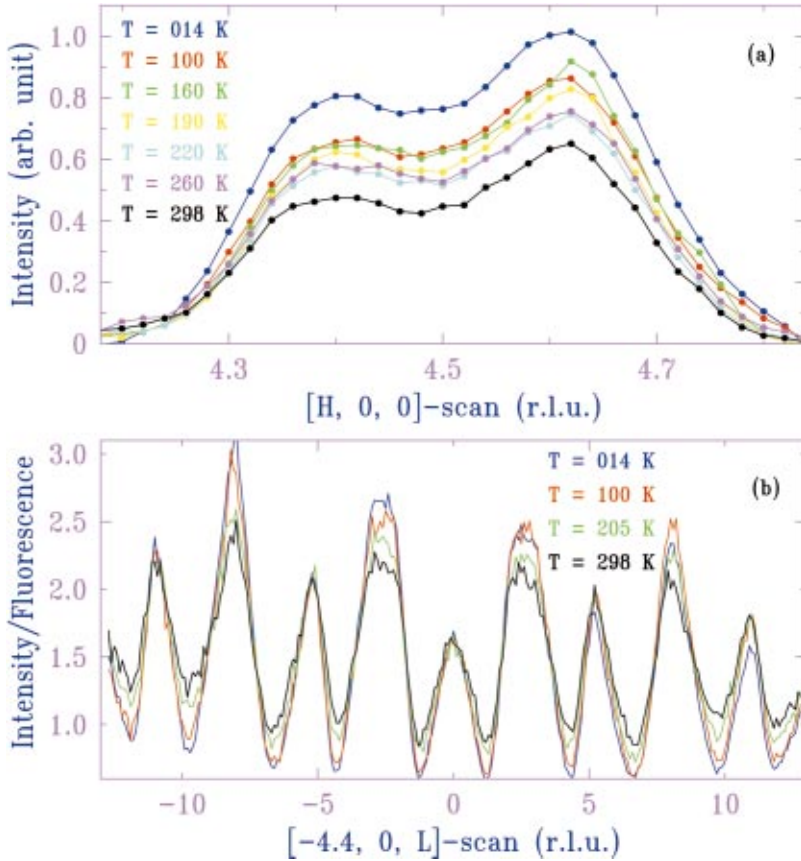


FIG. 3. (Color) (a) Diffuse scattering at various temperatures. The background including the TDS has been removed from the data. (b) L modulations of the $(-4.4, 0, 0)$ diffuse peak at selected temperatures. The intensity modulations are clearly enhanced as T is lowered.

The measurements of the diffuse peaks after subtracting background at various temperatures are shown in Fig. 3(a). The background, of which the thermal diffuse scattering (TDS) is the principal component, was modeled using Lorentzian tails emanating from the nearest Bragg points (which reproduce the expected asymptotic $1/q^2$ behavior of the TDS scattering in the vicinity of the observed peaks) and a linear term to take into account other weakly Q -dependent background contributions, respectively (see Fig. 1). The diffuse scattering shows a clear indication of increase at low T . Interestingly, Fig. 3(a) also indicates the presence of two temperature regions, ~ 100 – 160 and ~ 220 – 260 K, respectively, where there are no significant differences in the integrated intensity (proportional to the area under the curve) with temperature.

Figure 4(a) summarizes the temperature dependence of the diffuse scattering. We have included the data above 300 K from Ref. 14 to illustrate the expected behavior in the higher- T region, inaccessible in our measurements. Since the data from Ref. 14 were for oxygen stoichiometry of 6.67 with an ordering T of 323 K, we have shifted the temperature down by 10 K to be consistent with the transition temperature, $T_{oo} \sim 313$ K, for our composition. As shown, the intensity gradually increases on lowering T and becomes nearly constant in the ~ 220 – 260 -K range. Below $T_1 \sim 220$ K, however, the intensity starts to rise beyond the extrapolation (tildes) of the 220–260-K intensity, until $T_2 \sim 160$ K below which it seems to level off. Then, as the superconducting state is approached, the intensity gradually starts to rise again

and appears to saturate in that phase. The inset shows the intensity after subtracting the 220–260-K value.

By scanning along the \mathbf{c}^* axis in reciprocal space through the peaks at \mathbf{q}_0 , we see strong modulations as a function of Q_z (see Fig. 2), the significance of which was not fully appreciated^{13,21} until now. This intensity modulation is not purely sinusoidal suggesting that the displacements on more than two scattering planes are correlated along the \mathbf{c} axis. If we describe the scattering due to atomic displacements ($\parallel \mathbf{a}$) in a given layer $n(\perp \mathbf{c})$ by a complex structure factor F_n , then the intensity modulation along \mathbf{c}^* of the diffuse peak at $\mathbf{Q} = (Q_x, 0, Q_z)$ is given by

$$I(Q_z) = C Q_x^2 \left(\sum_{n, n'} \langle F_n F_{n'}^* \rangle e^{-i Q_z (z_n - z_{n'})} \right),$$

where z_n is the height along the \mathbf{c} axis of layer n . So, the separations along the \mathbf{c} axis of the correlated planes can be obtained by a direct Fourier transform of the intensity modulation. As shown in Fig. 2 (bottom panel), there are two planar distances, $z_1 = 0.362 \pm 0.008 c$ and $z_2 = 0.187 \pm 0.008 c$, respectively, that are correlated. z_1 corresponds to the distance between the CuO_2 and CuO_x chain planes, whereas z_2 is consistent with both the CuO_2 - O_{apical} (O_{apical} is the oxygen in between Cu(1) and Cu(2) atoms, respectively, along the \mathbf{c} axis) and the chain-Ba distances, respectively.⁸ Note that the correlation between the CuO_2 plane and CuO_x chain (z_1) is clearly much stronger. Figure 3(b) shows the behavior of the modulations at various temperature whereas Fig. 4(b) displays the temperature dependence of the corre-

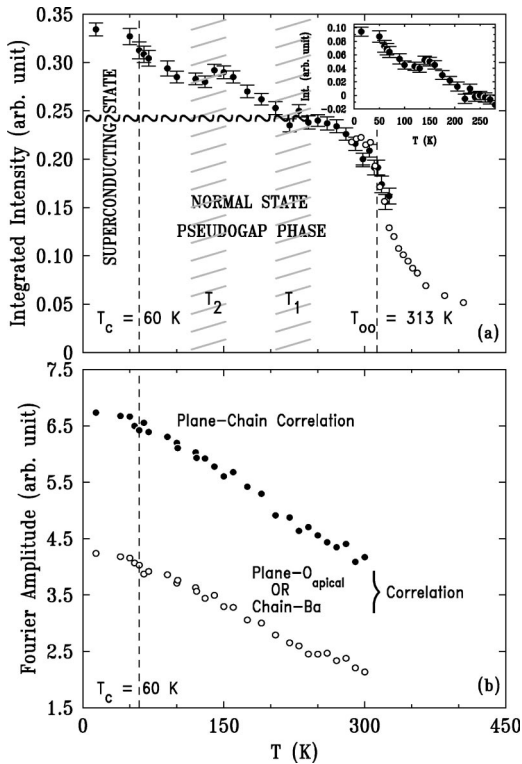


FIG. 4. (a) T dependence of the diffuse scattering at $(4.4, 0, 0)$. (\circ) are data from Andersen *et al.* (see the text) normalized to overlap with our data for 300–328 K. (\sim) depict low- T extrapolation of the intensity between ~ 220 –260 K. Hatched areas identify T regions where breaks in the intensity are observed. Inset: “Order parameter” of the charge stripes. (b) T dependence of the correlations.

lations. As shown, the Fourier amplitudes of z_1 and z_2 clearly grow at low T and appear to saturate in the superconducting state. Within our experimental uncertainties, we did not observe any changes in z_1 or z_2 .

In summary, our experiments showed that the diffuse peaks corresponding to $\mathbf{q}_0 = (\sim \frac{2}{5}, 0, 0)$ originate from mutually coupled, primarily longitudinal atomic displacements ($\delta \mathbf{u} \parallel \mathbf{a}$) of the CuO_2 , CuO_x chain, and O_{apical} and/or Ba, respectively. The primary result of our study is the unconventional T dependence of this diffuse scattering below ~ 220 K, which roughly corresponds to the temperature of entry into the “pseudogap” phase in this material. In addition, there appears to be a plateau at T_2 . Recent ion-channeling measurements observed similar characteristic temperatures in the T -dependence of incoherent atomic displacements in underdoped YBCO.²² Interestingly, μSR and neutron-diffraction studies^{23,24} on underdoped YBCO suggested the onset of a d -density-wave order²⁵ below T_2 . Another possibility is that below T_1, T_2 , and T_c different branching phases¹⁶ become stable, which does not seem very likely although we can not completely rule that out, as discussed above.

In conclusion, we propose that the lattice modulations observed in underdoped YBCO become strongly correlated with instabilities (i.e., charge fluctuations) in the CuO_2 planes that grow into the pseudogap phase. The charge fluctuations or stripes use oxygen-ordered superstructure as a spatial template. Figure 4 shows how the “order parameter” of such a stripe phase may evolve as the pseudogap phase and the superconducting state, respectively, are entered. In this connection we note that recent elastic neutron-diffraction work on a single, crystal YBCO sample²⁶ showed a peak at $\mathbf{q}_{\text{spin}} = (\sim 0.2, 0, 0)$. The absence of this peak in the x-ray scattering leads us to speculate that this peak is in fact due to the magnetic stripe corresponding to our observed scattering at twice this wave vector, i.e., $\mathbf{q}_0 = 2\mathbf{q}_{\text{spin}}$, and is also commensurate with the oxygen ordering in the chain planes.

The Advanced Photon Source is supported by the U.S. DOE, Office of Basic Energy Sciences (Contract No. W-31-109-ENG-38). We thank J. Almer for his help with the Weissenberg camera. We have greatly benefited from discussions with S. C. Moss, D. de Fontaine, and A. Paulikas.

*Email address: zahir@aps.anl.gov

¹T. Timusk and B. Statt, Rep. Prog. Phys. **62**, 61 (1999).

²B. Batlogg and C. M. Varma, Phys. World **13** (2), 33 (2000).

³S. Chakravarty *et al.*, Phys. Rev. B **61**, 14 821 (2000).

⁴J.M. Tranquada *et al.*, Phys. Rev. B **54**, 7489 (1996); also see Nature (London) **375**, 561 (1995).

⁵M.v. Zimmermann *et al.*, Europhys. Lett. **41**, 629 (1998).

⁶H.A. Mook *et al.*, Nature (London) **395**, 145 (1998); **404**, 729 (2000); P. Dai *et al.*, Phys. Rev. Lett. **80**, 1738 (1998); Phys. Rev. B **63**, 054525 (2001); M. Arai *et al.*, Phys. Rev. Lett. **83**, 608 (1999).

⁷H.A. Mook and F. Doğan, Nature (London) **401**, 145 (1999).

⁸J.D. Jorgensen *et al.*, Phys. Rev. B **41**, 1863 (1990).

⁹R. McCormack *et al.*, Phys. Rev. B **45**, 12 976 (1992); B.W. Veal and A.P. Paulikas, Physica C **184**, 321 (1991); H.F. Poulsen *et al.*, Nature (London) **349**, 594 (1991); J.M. Tranquada *et al.*, Phys. Rev. B **38**, 8893 (1988); J.D. Jorgensen *et al.*, *ibid.* **36**, 5731 (1987).

¹⁰J.D. Jorgensen *et al.*, Phys. Rev. B **36**, 3608 (1987).

¹¹C. Chaillout *et al.*, Phys. Rev. B **36**, 7118 (1987).

¹²R. Beyers *et al.*, Nature (London) **340**, 619 (1989); D.J. Werder *et al.*, Phys. Rev. B **37**, 2317 (1988).

¹³V. Plakhty *et al.*, Solid State Commun. **84**, 639 (1992).

¹⁴N.H. Andersen *et al.*, Physica C **317-318**, 259 (1999).

¹⁵F. Yakhou *et al.*, Physica C **333**, 146 (2000).

¹⁶D. de Fontaine *et al.*, Nature (London) **343**, 544 (1990); J. Less-Common Met. **168**, 39 (1991); Europhys. Lett. **19**, 229 (1992); G. Ceder *et al.*, Phys. Rev. B **41**, 8698 (1990).

¹⁷S. Yang *et al.*, Physica C **193**, 243 (1992).

¹⁸S.J. Rothman *et al.*, Phys. Rev. B **44**, 2326 (1991); **40**, 8852 (1989); X.M. Xie *et al.*, *ibid.* **40**, 4549 (1989).

¹⁹B.W. Veal *et al.*, Phys. Rev. B **42**, 6305 (1990).

²⁰T. Zeiske *et al.*, Physica C **194**, 1 (1992).

²¹P. Schleger *et al.*, Physica C **241**, 103 (1995).

²²R.P. Sharma *et al.*, Nature (London) **404**, 736 (2000).

²³J.E. Sonier *et al.*, Science **292**, 1692 (2001).

²⁴H.A. Mook *et al.*, Phys. Rev. B **64**, 012502 (2001).

²⁵S. Chakravarty *et al.*, cond-mat/0112109 (unpublished); cond-mat/0101204 (unpublished).

²⁶M. Arai *et al.*, Int. J. Mod. Phys. B **14**, 3312 (2000).